Earthquakes and Structures, *Vol. 9, No. 1 (2015) 257-279*
DOI: http://dx.doi.org/10.12989/eas.2015.9.1.257

Developing fragility curves and loss functions for masonry infill walls

Donatello Cardone* and Giuseppe Perrone

School of Engineering, University of Basilicata, Viale Ateneo Lucano 10, 85100 Potenza, Italy

(Received February 9, 2015, Revised May 30, 2015, Accepted May 30, 2015)

Abstract. The primary objective of this study is to summarize results from previous experimental tests on laboratory specimens of RC/steel frames with masonry infills, in order to develop fragility functions that permit the estimation of damage in typical non-structural components of RC frame buildings, as a function of attained peak interstory drift. The secondary objective is to derive loss functions for such non-structural components, which provide information on the probability of experiencing a certain level of monetary loss when a given damage state is attained. Fragility curves and loss function developed in this study can be directly used within the FEMA P-58 framework for the seismic performance assessment of RC frame buildings with masonry infills.

Keywords: masonry infills; damage states; fragility functions; repair costs; loss functions; FEMA P-58

1. Introduction

Reinforced Concrete (RC) frame buildings with non-structural masonry infill walls are common building systems worldwide. Past earthquakes have shown that economic losses in typical RC frame buildings, after minor and moderate seismic events, are strongly influenced by damage to masonry infills and partitions. Such non-structural components often experience significant damage during earthquakes, due to their in-plane and out-of-plane fragile behavior, which may also pose a huge threat to human lives.

One of the most promising approaches for estimating (hence reducing) losses resulting from an earthquake is Performance-Based Earthquake Engineering (PBEE) (Bozorgnia and Bertero 2004). Recently, the US Federal Emergency Management Agency (FEMA) contracted with the Applied Technology Council (ATC) the development of a seismic performance assessment methodology. The work was completed in 2012 with the publication of a series of volumes collectively referred to as FEMA P-58 (ATC 2012a, b). For practical implementation of the methodology, work included the development of an electronic tool, referred to as the Performance Assessment Calculation Tool (PACT). The PBEE approach implemented in FEMA P-58 appears to be very attractive and promising, because it utilizes performance measures that can be understood by decision makers. In FEMA P-58, indeed, future seismic performance of buildings is expressed in

*Corresponding author, Professor, E-mail: donatello.cardone@unibas.it

http://www.techno-press.org/journals/eas&subpage=7 ISSN: 2092-7614 (Print), 2092-7622 (Online)

terms of repair costs, fatalities, and repair time (dollars, deaths, and downtime).

In the probabilistic framework of FEMA P-58, estimation of economic losses is performed in three steps. In the first step, a probabilistic description of the structural response at increasing levels of seismic intensity is obtained through nonlinear response history analyses. In the second step, damage to individual structural and non-structural components is estimated as a function of structural response parameters (e.g., peak interstory drifts) computed in the first step. This requires fragility functions for various damage states for each component type in the facility. In the third step, economic losses to individual components are estimated as a function of the level of damage sustained by the component. This requires loss functions for various damage states for each component in the facility. At the moment, specific tools (i.e., fragility curves and loss functions) for the PBEE analysis of non-structural masonry infill walls are missing. This study represents a first step towards filling this gap, developing fragility curves and loss functions for masonry infill walls, which can be implemented in PACT for PBEE analysis.

2. Fragility groups

Three different Fragility Groups (FGs) are identified for masonry infill walls, i.e., (i) Exterior masonry Infill Walls without openings (EIW), (ii) Exterior masonry Infill Walls with Windows (EIW_w) and (iii) Exterior masonry Infill Walls with French Windows (EIW_fw). In addition, two FGs are defined for interior partitions, i.e., (iv) Interior partitions without openings (IP) and (v) Interior partitions with Doors (IP_d), although no specific tests on masonry partitions have been carried out so far.

The expected behavior under monotonic or cyclic loading of masonry infill walls is first examined, to identify typical crack/damage patterns, to be considered for repair interventions in the evaluation of the loss functions.

Due to the lack of results from laboratory tests on not-infilled masonry partitions, in the first approximation, the experimental results relevant to masonry infills are assumed valid also for masonry partitions, even when they are not inserted in a RC frame. It is worth noting that this assumption is on the safe side, as the deformation limits for masonry non-infills are expected to be a little greater than for infills (Sucuoglu 2013).

3. Definition of damage states

For each FG, a number of damage states (DSs) have been defined to characterize damage development in masonry infill walls. Damage states are defined by observations on extent and severity of cracking, failure of brick units, damage on frames (windows, French windows and doors), etc., supported and/or complemented by other macroscopic damage indicators, such as the attainment of the peak force or given strength reduction ratios. In particular, four discrete DSs are defined for each FG, based on specific repair actions that would have to be taken as a result of the observed damage. This approach facilitates the estimation of economic losses and other types of consequences (e.g., repair time, etc.) resulting from the occurrence of damage. The selected damage states can be generally described as follows:

• ***DS1 (Light Cracking).*** At DS1, damage results in detachment of the masonry panel from the RC frame, at the intrados of the top beam and along the upper half-height of the columns. Light

diagonal cracking of the infill (1-2 cracks with width <1 mm) in both directions may also occur.

• ***DS2 (Extensive cracking).*** At DS2, the cracks developed at DS1 widen (1 mm<width<2 mm). In addition, new diagonal cracks are expected to form in both directions (25-35% of the panel area is assumed to be affected by cracks at DS2). Possible failure of some brick units, located on the upper corners and top edge of the infill (corresponding to 10% of the panel area), is expected.

• ***DS3 (Corner crushing).*** At DS3, detachment of large plaster area and significant sliding in the mortar joints are expected to occur. In addition, crushing and spalling of brick units are more widespread on the panel (30% of the panel area is assumed to be affected by crushing/spalling of bricks). The wall is not repairable at reasonable costs (it is more convenient to demolish and reconstruct the entire wall). Frames (if any) are not damaged and can be retrieved and re-installed.

• ***DS4 (Collapse).*** DS4 corresponds to the in-plane or out-of-plane (whichever occurs first) global collapse of the wall. Frames (if any) are damaged and cannot be retrieved and used again.

It is worth noting that, in the first approximation, the same damage states have been assumed for interior partitions, with the only exception of DS4 that has been assumed coincident with DS3, due to the inherent higher fragile behavior of partitions at collapse. Damage states for exterior infills and interior partitions are summarized in Table 1.

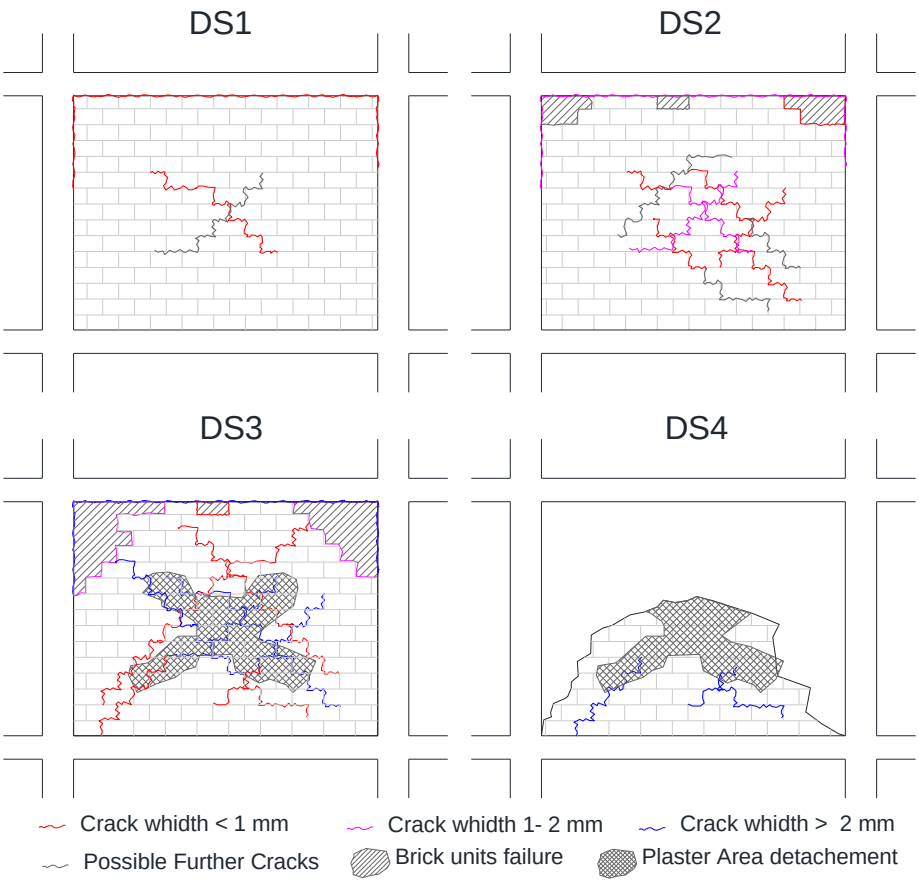

Fig. 1 Damage states of masonry infills without openings

Table 1 Description of damage states for masonry walls considered in this study

Fragility group	Damage states
Masonry walls w/o openings	DS1: Separation of the infill from the frame (top beam and mid-height columns), light diagonal cracking (width<1 mm)
	DS2: Extensive diagonal cracking (1 mm<width<2 mm), possible failure of brick units
	DS3: Corner crushing, brick spalling, detachment of large plaster area, sliding in the mortar joints. Collapse of interior partitions.
	DS4: In-plane or out-of-plane collapse of exterior infills.
Masonry walls with openings	DS1: Separation of the infill from the frame (top beam and columns), light diagonal cracking (width<1 mm)
	DS2: Extensive diagonal cracking (1 mm<width<2 mm), possible failure of brick units
	DS3: Corner crushing, brick spalling, detachment of large plaster area, sliding in the mortar joints. Collapse of interior partitions.
	DS4: In-plane or out-of-plane global collapse of exterior infills (frame included).

4. Experimental results used in this study

Interstory drift ratio (IDR) has been chosen as engineering demand parameter to describe the evolution of in-plane damage due to earthquake loading in masonry infill walls (and partitions). Peak floor accelerations (PFA) have been chosen as engineering demand parameters to identify the out-of-plane collapse of masonry infill walls (and partitions).

Generally speaking, in many cases, there was not enough information to establish the interstory drifts at which each damage state takes place. This occurs either because the damage state did not occur or because the research report does not document in detail information to properly establish the level of interstory drift at which the damage state was observed. As a matter of fact, only a number of investigations have reported detailed information about cracking patterns and crack widths at various levels of lateral deformation. Therefore, in order to gather more data points associated with the first and second damage state, when no specific information on crack patterns and crack widths were available, it was assumed that DS2 occurs at interstory drifts at which the peak strength in the hysteresis loop was attained. In these circumstances, DS1 was deemed to occur at interstory drifts equal to 2/3 those associated with DS2. This approach was followed only when detailed hysteresis loops were recorded. Similar problems were faced when trying to determine the interstory drifts associated with the third and fourth damage state. As a consequence, in order to expand the number of data points associated with these DSs, when no specific information from the investigators were available, reference to the interstory drifts at which a strength loss in the skeleton curve of the order of 20% and 50%, respectively, was observed, has been made.

Information about material properties and characteristics of all the masonry infill specimens considered in this study is summarized in Table 2, which includes results from 19 different experimental investigations on 55 laboratory specimens. Basically, two types of specimens have to be distinguished (see column labeled with “Opening” in Table 2), i.e., specimens without openings

and specimens with door or window opening. Tests include in-plane monotonic, cyclic, pseudo-dynamic and shaking table tests, as well as a number of out-of-plane monotonic and shaking table tests. In Table 2, information on masonry unit and mortar type utilized for each specimen is summarized, together with an estimate of the average compressive strength of masonry (f_{wm}). In addition, the slenderness ratio (H/s), aspect ratio (H/L) and opening ratio (A'/A) of each specimen are reported, where H, L and s indicate the height, width and thickness of the masonry panel, respectively, A is the area of the masonry panel and A' is the area of the door/window. The reference paper/report for each experimental investigation is indicated in the second column of Table 2.

Table 3 presents the interstory drift ratios associated with the four in-plane damage states considered in this study. Interstory drifts associated with the attainment of DS1 exhibit a large dispersion, being reported to occur for interstory drifts as small as 0.06% or as large as 0.46%. Based on the available experimental data, DS2 and DS3 occur at interstory drifts ranging from 0.21% to 1.38% and from 0.5% to 1.98%, respectively. Finally, DS4 is reported to occur from interstory drift as low as 1.06% to as high as 3.26%. Quite surprisingly, negligible differences, in terms of damage evolution and interstory drifts associated to specific damage states, are observed for masonry infills with and without openings. For that reason, in the first instance, all the available data are put together and used to develop first-attempt in-plane fragility curves for masonry infills without opening, that represent the majority of the specimens tested (see Table 2). Another approximation comes from using directly the interstory drift recorded experimentally, neglecting the differences between the test specimens in terms of aspect ratio. A more rational approach could be that of defining an equivalent diagonal strain for each specimen, thus taking into account the differences in terms of aspect ratio between one specimen and another, and then developing fragility curves in terms of equivalent strain rather than interstory drift. Always in the first approximation, the fragility curves for masonry infills with openings are tentatively derived from those relevant to masonry infills without opening, based on the considerations discussed in the next section. In the last column of Table 3, the peak floor accelerations corresponding to out-of-plane collapse of masonry infills, previously damaged in their plane (basically according to DS2), are reported. Based on the available experimental data, the out-of-plane collapse of masonry infills is expected to occur for peak floor accelerations ranging from 0.2 g to 0.8 g.

Table 2 Properties of masonry infill specimens considered in this study

N.	Reference	Label	Masonry unit (*)	Mortar type	H/s	H/L	f_{wm} (MPa)	Opening	A'/A	Loading type (**)
1	Angel *et al.* (1994)	2a	Cl_Br	Type N	34	0.6	10.85	none	-	IN (C) OUT (M)
2		3a	Cl_Br	Lime	34	0.6	10.13			
3		6a	Co_Bl	Lime	17	0.6	4.58			
4		7a	Co_Bl	Type N	17	0.6	11.0			
5		8a	Co_Bl	Lime	9	0.6	3.50			
6	Paulo Pereira *et al.* (2011)	WR	H_Cl_Br	M5	11.3	0.48	10.5	none	-	IN (C) OUT (M)
7	Calvi *et al.* (2004)	NR2	H_Cl_Br	M5	20.4	0.65	1.1	none	-	IN (C) OUT (M)

Table 2 Continued

N.	Reference	Label	Masonry unit (*)	Mortar type	*H*/*s*	*H*/*L*	f_{wm} (MPa)	Opening	*A'*/*A*	Loading type (**)
8		NR6			20.4	0.65	1.1			
9	Carydis *et al.* (1992)	1	H_Cl_Br	-	31.2	0.83	18.2	none	-	OUT (S)
10		2			31.2	0.83	18.2			
11	Colangelo (2003)	C1	H_Cl_Br	Cement-Lime	10.8	0.76	4.22	none	-	IN (P)
12		C2			10.8	0.76	4.57			
13		L1			10.8	0.56	4.01			
14		L2			10.8	0.56	4.37			
15		N1			16.2	0.56	3.46			
16		N2			16.2	0.56	3.71			
17	Pires and Carvalho (1992)	M6	H_Cl_Br	M5	10.6	0.7	2.2	none	-	IN (C)
18	Meherabi *et al.* (1996)	3	S_Cl_Br	M15	14.2	0.67	15.1	none	-	IN (M)
19		4	H_Cl_Br		14.2	0.67	10.6			IN (C)
20		5	S_Cl_Br		14.2	0.67	13.8			IN (C)
21		6	H_Cl_Br		14.2	0.67	10.1			IN (C)
22		7	S_Cl_Br		14.2	0.67	13.6			IN (C)
23		8	H_Cl_Br		14.2	0.67	9.5			IN (M)
24		9	S_Cl_Br		14.2	0.67	14.2			IN (M)
25		10	H_Cl_Br		14.2	0.48	10.6			IN (C)
26		11	S_Cl_Br		14.2	0.48	11.4			IN (C)
27		12	S_Cl_Br		14.2	0.48	13.6			IN (C)
28	Manos *et al.* (1995)	-	-	-	-	-	-	none	-	IN
29	Zarnic (1995)	-	-	-	-	-	-	none	-	IN
30	Kappos *et al.* (1998)	1	Cl_Br	-	15	0.5	1.5	none	-	IN (C)
31		2			15	0.5	3.0	none	-	
32	Pujol *et al.* (2008)	-	S_Cl_Br	Type N	30.4	0.5	1.9	none	-	IN (C)
33	Zarnic and Gostic (1997)	-	-	-	-	-	-	none	-	IN
34	Negro and Verzelletti (1996)	2	H_Cl_Br	M5	18	0.58 0.875	7.3	none	-	IN (P)
35	Zarnic and Tomasevic (1984)	M2	S_Cl_Br	M10	12.5	0.75	15.2	none	-	IN (C)
36	Mosalam *et al.* (1997)	S2-N	Co_Bl	M10	16.5	0.52	16.5	none	-	IN (C)
37		S2-A		M10	16.5	0.52	16.5	door	0.107	

Table 2 Continued

N.	Reference	Label	Masonry unit (*)	Mortar type	*H/s*	*H/L*	f_{wm} (MPa)	Opening	*A'/A*	Loading type (**)
38		S2-S		M15	16.5	0.52	22.8	window	0.053	
39	Schneider *et al.* (1998)	40W2	S_Cl_Br	Type N	8	1	6.9	window	0.35	IN (C)
40		60W1			8	1	7.3	window	0.175	
41		60W2			8	1	7.1	window	0.175	
42		80W1			8	1	6.5	none	-	
43	Tasmini and Mohebkhah (2011)	SW	Cl_Br	M10	16.4	0.79	7.4	none	-	IN (C)
44		PW1			16.4	0.79	7.4	window	0.061	
45		PW2			16.4	0.79	7.0	window	0.137	
46		PW3			16.4	0.79	7.0	window	0.177	
47		PW4			16.4	0.79	8.5	door	0.249	
48	Sigmund and Penava (2012)	1I	H_Cl_Br	M5	15	1	2.7	door	0.097	IN (C)
49		2I			15	1	2.7	window	0.092	
50		3I			15	1	2.7	door	0.097	
51		4I			15	1	2.7	window	0.092	
52		2III			15	1	2.7	none	-	
53	Kakaletsis and Karayannis (2008)	S	H_Cl_Br	M1	13.3	0.67	2.63	none	-	IN (C)
54		WO2			13.3	0.67	2.63	window	0.093	
55		DO2			13.3	0.67	2.63	door	0.20	

(*)Cl_Br: Clay Brick ;Co_Bl: Concrete Blok; H_Cl_Br: Hollow Clay Brick S_Cl_Br: Solid Clay Brick
(**)IN: In plane; OUT: out of plane; (C) Cyclic; (M) Monotonic; (P) Pseudodynamic; (S) Shaking table

5. Evaluation of fragility functions

As shown in Table 3, the interstory drift ratio at which each damage state is reported to occur shows important variations from one specimen to another. In order to estimate how likely it is that a given damage state will occur in a RC frame undergoing a specific level of drift, it is necessary to take into account this specimen-to-specimen variability. This uncertainty can be explicitly taken into account by developing drift-based fragility functions.

Drift-based fragility functions provide information about the probability of experiencing (or exceeding) a particular damage state as a function of the peak interstory drift ratio experienced by the masonry infill wall. In other words, they provide the probability of experiencing or exceeding a particular damage state conditioned on the peak interstory drift.

Usually, fragility functions take the form of lognormal cumulative distribution functions, having a median value, θ, and logarithmic standard deviation, or dispersion, β. The mathematical form for such a fragility function is

$$F_i(DS > ds_i | d = IDR) = \Phi\left(\frac{\ln(d/\theta_i)}{\beta_i}\right) \quad (1)$$

Table 3 Interstory drift ratios (IDR) and Peak floor accelerations (PFA) used to develop fragility functions for masonry infill walls

N.	IDR_{DS1} (%)	IDR_{DS2} (%)	IDR_{DS3} (%)	IDR_{DS4} (%)	PFA_{DS4} (g)	N.	IDR_{DS1} (%)	IDR_{DS2} (%)	IDR_{DS3} (%)	IDR_{DS4} (%)	PFA_{DS4} (g)
1	0.195	0.39	-	-	0.52	29	0.1	0.3	-	-	-
2	0.125	0.25	-	-	0.78	30	0.08	0.36	-	-	-
3	0.109	0.218	-	-	0.8	31	0.06	0.27	-		-
4	0.172	0.344	-	-	0.68	32	0.15	-	-	1.75	-
5	0.125	0.25	-	-	0.6	33	0.2	-	-	-	-
6	0.1	0.355	0.6	-	0.7	34	-	-	1.1	-	-
7	0.2	0.4	1.2	-	0.2	35	0.2	-	-	2	-
8	0.185	0.415	-	-	0.6	36	-	0.69	-	1.86	-
9	-	-	-	-	0.45	37	-	0.8	-	2.54	-
10	-	-	-	-	0.8	38	-	0.58	-	3.26	-
11	-	0.43	-	1.42	-	39	-	-	1.38	2.25	-
12	-	1.06	-	1.06	-	40	-	-	1.07	1.5	-
13	-	1.38	-	1.63	-	41	-	-	1.2	1.75	-
14	-	1.1	-	2.28	-	42	-	-	0.93	1.5	-
15	-	0.8	-	2.03	-	43	-	-	1.1	2.7	-
16	-	0.84	-	2.16	-	44	-	-	0.8	2.4	-
17	0.1	-	-	-	-	45	-	-	0.8	1.9	-
18	0.21	0.21	1.16		-	46	-	-	0.8	2.6	-
19	0.17	0.63	1.24		-	47	-	-	0.79	2.5	-
20	0.33	0.79	1.4		-	48	0.19	0.35	0.5	-	-
21	0.36	0.61	0.91		-	49	0.18	0.49	1.29	-	-
22	0.46	0.71	0.82		-	50	0.18	0.57	0.93	-	-
23	0.2	0.91	1.59		-	51	0.22	0.58	1.3	-	-
24	0.33	0.48	1.98	-	-	52	0.16	0.42	1.09	-	-
25	0.17	0.4	0.91	-	-	53	0.28	0.92	-	-	-
26	0.36	0.74	0.91	-	-	54	0.38	1.11	-	-	-
27	0.17	0.55	0.66	-	-	55	0.27	1.2	-	-	-
28	0.15	0.3	-	2	-						

where $F_i(\mathrm{DS}>ds_i|d=\mathrm{IDR})$ is the conditional probability that the component will experience or exceed the i-th damage state as a function of the attained interstory drift, d; Φ denotes the standard normal (Gaussian) cumulative distribution function; θ_i is the median value of the probability distribution of drift ratios (i.e., the value of demand at which there is a 50% probability that a component will reach or exceed that damage state) and β_i is the logarithmic standard deviation, which accounts for uncertainty in the value of demand at which a component reaches a given damage state. To establish θ_i and β_i for each component type and damage state, the procedure described below has been followed.

In the first step, cumulative frequency distributions of interstory drift ratios corresponding to the each damage state have been obtained by plotting ascending-ordered drift ratios at which each damage state was experimentally observed to occur against (i-0.5)/n, where "i" is the position of the drift ratio in the ordered list of drift ratios and "n" is the number of specimens in which the drift associated with that damage state was identified. These cumulative frequency distribution functions provide information about the portion of the data set corresponding to each damage state that does not exceed a particular value of drift and represent empirically derived cumulative distribution functions.

In the second step, the ordered data have been revised to eliminate possible outliers from the bulk of data (i.e., values of drift that result significantly above or below θ_i). Indeed, it is possible that one or more tests have reported spurious values of demand that reflect experimental errors or misinterpretation of experimental results rather than true values of drift at which the specimen attained a given DS. According to the Annex H of FEMA P-58 (2012a), the Peirce's criterion (Ross 2003) has been applied to test and eliminate doubtful observations of interstory drift ratio. As a matter of fact, only one point (at DS4) has been eliminated.

In the next step, the Method of Maximum Likelihood has been used to fit cumulative probability functions to the final data sets, assuming that the data were lognormally distributed. According to this method, the median value of the demand at which a given damage state is likely to initiate, θ_i, can be computed with the following equation

$$\theta_i = \exp\left(\frac{1}{N}\sum_{j=1}^{N}\ln\left(d_j\right)\right) \tag{2}$$

where N is the total number of data, d_j is the drift ratio in the j-th test at which the damage state under consideration occurs.

For experimental tests in which specimens were subjected to slowly increasing displacement demand and where the interstory drift ratio corresponding to the onset of a given damage state was actually recorded or properly documented by the investigators, d_j is the observed data.

For experimental tests where specimens were subjected to increments of displacement demand, and the damage state was observed in the first cycle of the next demand increment, d_j is the interstory drift ratio at the midpoint of the demand increment that caused the attainment of that damage state.

The value of the random dispersion, $\beta_{r,i}$ for the i-th DS, is given by

$$\beta_{r,i} = \sqrt{\frac{1}{N-1}\sum_{j=1}^{N}\left(\ln\left(\frac{d_j}{\theta_i}\right)\right)^2} \tag{3}$$

where N, d_j, and θ_i are as defined above. It is worth noting that the computed values θ and β_r are approximately, but not exactly, equal to the median and c.o.v. for each data set.

In the next step, Lilliefors goodness-of-fit testing (Lilliefors 1967) was carried out to verify the assumption of the lognormal distribution and evaluate the accuracy of the fragility parameters derived in the previous step. In accordance with Annex H of FEMA P-58 (2012a), the fragility parameters have been deemed acceptable if the Lilliefors test passes, considering a 5% significance level.

In the last step, the computed distribution parameters have been adjusted to facilitate application in practice and account for uncertainty associated with the size of the data sets and

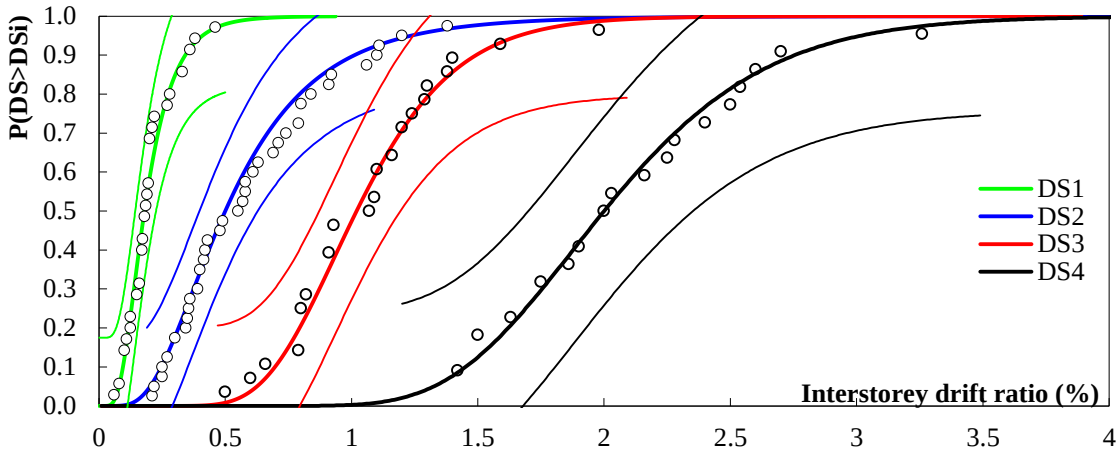

Fig. 2 Fragility functions fitted to interstory drift ratios associated with in-plane DSs of masonry infills without openings

differences between tests and actual building behavior, as discussed in detail in the following.

Fig. 2 shows the empirical cumulative distribution functions for the four in-plane DSs of masonry infills without openings. Also plotted in the graphs of Fig. 2 are the fitted lognormal cumulative distribution functions of the interstory drifts. As can be seen, the lognormal distributions fit the data relatively well. Also shown in Fig. 2 are graphical representations of Lilliefors goodness-of-fit tests for 5% significance levels. The hypothesis that the assumed cumulative probability distributions adequately fit the empirical data is accepted since all data points lie between the two thin lines representing the 5% significance interval.

The fragility function parameters for exterior masonry infills w/o openings are given in Table 4. The median values (θ) of interstory drift ratio have been rounded to the nearest 0.05% to facilitate use. Generally speaking, Fig. 2 points out that DS1 (light cracking) is not likely to be observed if the interstory drift is smaller than about 0.05% while it would be almost certain to occur if the peak interstory drift ratio is larger than 0.5%. Similarly, DS2 (extensive cracking) would not be likely to be observed if the peak interstory drift is smaller than 0.15%, but it is almost certain to occur if the peak interstory drift ratio exceeds 1%. DS3 (corner crushing) would be not expected to occur for interstory drifts less than 0.5%, while it is almost certain to occur for interstory drifts greater than 2%. Finally, DS4 (global collapse) is not likely to be observed if the interstory drift is smaller than about 1.25% while it would be almost certain to occur if the peak interstory drift ratio is larger than 3.5%.

As far as global collapse is concerned, the out-of-plane behavior must be checked, in order to determine the actual mode of collapse of masonry infills. Out-of-plane collapse fragility curve has been derived based on limited number of data, as shown in Table 3. The selected engineering demand parameter is the peak acceleration registered in the middle of the panel. In first approximation, however, it can be assumed equal to the peak floor acceleration recorded at the i-th storey of a building (where the considered masonry infill is built) during an earthquake.

Fig. 3 shows the empirical cumulative distribution function for the out-of-plane collapse of masonry infills without openings. Also plotted in the graphs of Fig. 3 is the fitted lognormal cumulative distribution function of the peak floor acceleration. As can be seen, the lognormal

distribution fit the data relatively well. In order to fully verify if the cumulative distribution function could be assumed as lognormally distributed, a Lilliefors goodness-of-fit test has been conducted. As can be seen in Fig. 3, the lognormal distribution adequately fit the empirical data since all data points lie between the two 5% significance lines.

The fragility function parameters associated to out-of-plane collapse of exterior masonry infills w/o openings are given in Table 4. The median value (θ) of peak floor acceleration results equal to 0.65 g and dispersion β_r is around 0.2. In the first approximation, the same fragility function parameters have been assumed for interior partitions w/o openings. Fig. 3 shows that out-of-plane collapse is not likely to be observed if the peak floor acceleration is smaller than about 0.35 g while it would be almost certain to occur if the peak floor acceleration is greater than 1 g.

The dispersion parameter β_u, which account for uncertainty associated with actual building conditions and lack of data, has been set equal to 0.25 according to the recommendations provided in Appendix H of FEMA P-58 (2012a). As a result, a total dispersion β equal to 0.35 has been obtained (see Table 4).

It is worth noting that the fragility curves shown in Figs. 2-3 have been derived processing all together the available experimental data (see Tab. 3), although they refer to different masonry types realized using different types of bricks and mortar (see Tab. 2). In this study, indeed, it has been chosen to keep all the data together, because an apparent separation between data relevant to different masonry types has not been observed. In the future, however, it would be desirable to particularize fragility curves for each masonry type. This may lead to some differences in the median values associated to each DS but probably also to lower dispersions.

Rough estimates of the fragility function parameters for masonry infills and partitions with openings have been obtained following the recommendations of Fajfar and Dolsek (2008), supported by the experimental results of pseudo-dynamic tests of partially infilled frames (Carvalho and Coelho 2001), which suggest, for masonry infills with openings, a reduction of the interstory drift corresponding to the attainment of the maximum strength (DS2 in this study) of the order of 25% in presence of windows and of the order of 50% in presence of doors. By analogy, the same reduction factor has been applied to the interstory drifts corresponding to first cracking

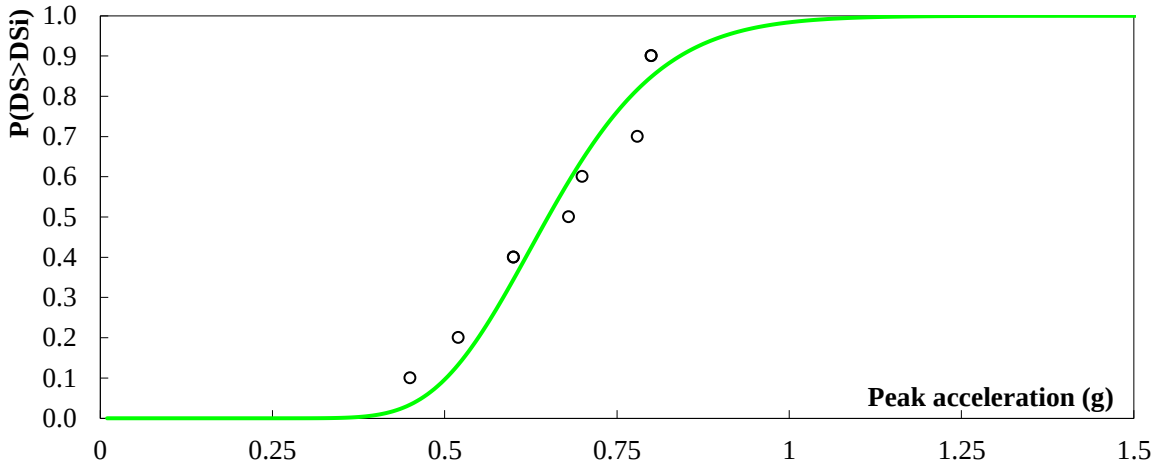

Fig. 3 Fragility function fitted to peak floor accelerations associated with out-of-plane collapse of masonry infills without openings

Table 4 Proposed fragility function parameters for performance-based seismic evaluation of masonry infills and partitions

Fragility group	Components	Damage States	Fragility function parameters			
			Median IDR(%), PFA (g)	Dispersion		
				β_r	β_u	β
Exterior and Interior(*) walls w/o openings	Masonry infills with French window and Partitions with door	Detachment of infill, Light diagonal cracking	0.15%	0.45	0.25	0.5
		Extensive diagonal cracking	0.40%	0.41	0.25	0.5
		Corner crushing and sliding of mortar joints	1.0%	0.26	0.25	0.4
		Global collapse	1.75% (a) 0.65g (b)	0.18(a) 0.21(b)	0.25	0.35
Exterior and Interior(*) walls with openings	Masonry infills with window	Detachment of infill, Light diagonal cracking	0.10%	0.45	0.25	0.5
		Extensive diagonal cracking	0.30%	0.41	0.25	0.5
		Corner crushing and sliding of mortar joints	0.75%	0.26	0.25	0.4
		Global collapse	1.75% (a) 0.65g (b)	0.18(a) 0.21(b)	0.25	0.35
	Masonry infills with french window and Partitions with doors	Detachment of infill, Light diagonal cracking	0.075%	0.45	0.25	0.5
		Extensive diagonal cracking	0.20%	0.41	0.25	0.5
		Corner crushing and sliding of mortar joints	0.50%	0.26	0.25	0.4
		Global collapse	1.75% (a) 0.65g (b)	0.18(a) 0.21(b)	0.25	0.35

(*)For interior partitions, DS3=DS4
(a)In-plane collapse, (b) Out-of-plane collapse

(DS1 in this study) and corner crushing (DS3 in this study), while the interstory drifts (and peak floor accelerations) associated to global collapse of masonry infills and partitions with openings have been assumed equal to those derived for masonry walls w/o openings, based on other experimental evidence (Tasnimi *et al.* 2011, Schneider *et al.* 1998). The medians of the interstory drift corresponding to the attainment of the four DSs in masonry infills (and partitions) with openings, obtained following the approach described before, are tentatively reported in Table 4. For simplicity, the same dispersion values have been assumed for masonry walls with and w/o openings. Fig. 4 compares the fragility curves relevant to masonry infills with and without openings. Obviously, further studies are needed to derive more accurate estimates of the fragility function parameters for masonry infills (and partitions) with openings.

The fragility functions developed before can be used to estimate the probability that a given masonry infill wall is at a specific in-plane damage state when it is subjected to a certain level of peak interstory drift. This probability can be estimated as the arithmetic difference between fragility functions corresponding to two consecutive damage states as follows

$$P\left(DS = ds_i, IDR_k\right) = \begin{cases} 1 - P\left(DS \geq ds_1 \middle| IDR = IDR_k\right) \\ P\left(DS \geq ds_1 \middle| IDR = IDR_k\right) - P\left(DS \geq ds_2 \middle| IDR = IDR_k\right) \\ P\left(DS \geq ds_2 \middle| IDR = IDR_k\right) - P\left(DS \geq ds_3 \middle| IDR = IDR_k\right) \\ P\left(DS \geq ds_4 \middle| IDR = IDR_k\right) \end{cases} \tag{4}$$

Fig. 5 shows the probability functions of being in each damage state for masonry infill panels without openings. For instance, for masonry infill walls experiencing 1% peak interstory drift, the probability of being in DS1 is 3.2%, 46.1% in DS2 and 45.0% in DS3 and 5.7% in DS4. At 3% drift, instead, the masonry panel for sure has experienced significant damage and there is a 7.9% probability that it is in DS2, 41.9% in DS3 and 50.0% in DS4. There is also a 0.2% probability that the panel has experienced light damage (DS1).

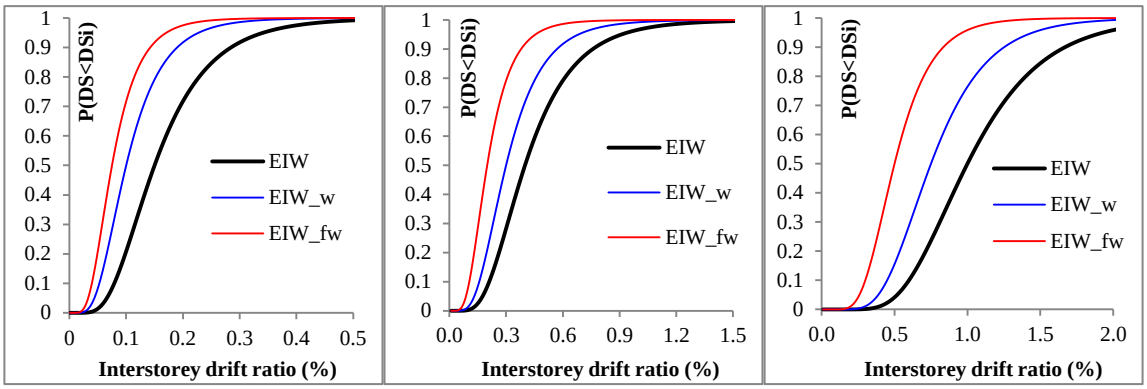

Fig. 4 Comparison between fragility curves of Exterior masonry Infill Walls without openings (EIW), with window (EIW_w) and with French window (EIW_fw) at (a) DS1, (b) DS2 and (c) DS3

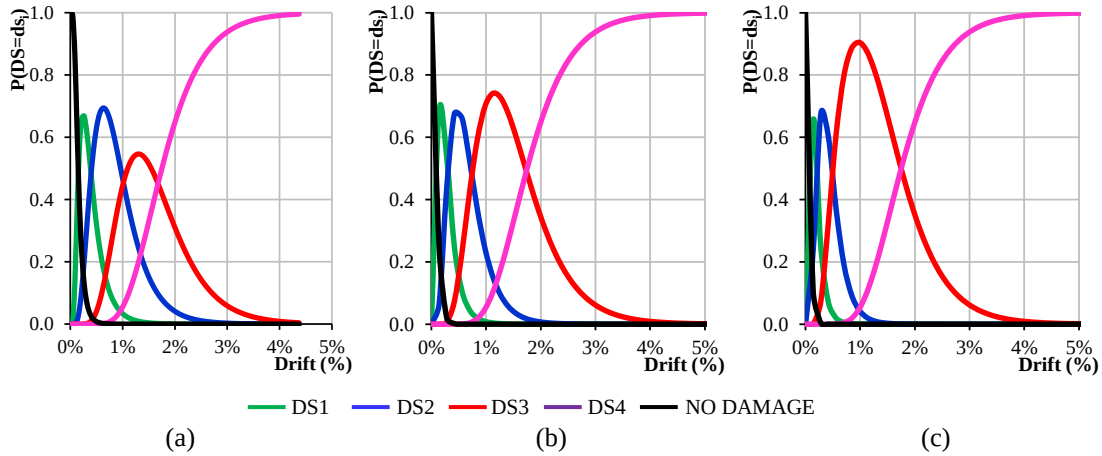

Fig. 5 Probability of being at each damage state for: (a) EIW, (b) EIW_w, (c) EIW_fw

6. Repair costs and loss functions

Economic losses associated with repair costs for damaged masonry infills can be expressed in terms of loss functions. Loss functions are defined as probabilistic estimates of the costs associated with the repair or replacement actions required in individual components when a specific damage state is reached. Loss function, therefore, provides information on the probability of experiencing a certain level of monetary loss when a given damage state is attained. In other words, they provide the probability of occurrence of a level of economic loss conditioned on the attainment of a given damage state in a component. Loss functions can be expressed, in a normalized form, as follows

$$l_j|DS_i = \frac{RC_j|DS_i}{a_j} \tag{5}$$

where $l_j|DS_i$ is the economic loss in the j-th component conditioned on the occurrence of the i-th damage state, $RC_j|DS_i$ is the repair cost for the j-th component when the i-th damage state has occurred; a_j is the replacement cost of the j-th component, i.e., the construction cost required to re-build the same component.

Economic losses are random variables. Based on the recommendations of FEMA P-58 (2012a, b), it can be assumed that economic losses follow a cumulative lognormal distribution. Unfortunately, poor information are available on the statistics of specific repair actions at the component level, as well as on the correlation coefficients between different repair actions corresponding to different

Table 5 Repair methods and repair activities for masonry infills and partitions

Damage States	Method of repair	Repair actions and associated preliminary and supplementary activities
DS1	Cosmetic repair and patch some cracks	Install scaffolding and shoring systems. Remove plaster along the upper (lateral) edge of the infill and across main diagonal cracks (a strip of 0.2 m width across each crack). Repair damaged area by patching new plaster using fiber-glass reinforcing mesh embedded in the base coat. Paint each side.
DS2	Patch some cracks	Install scaffolding and shoring systems. Remove furnishings, electrical and plumbing systems, as necessary. Demolish loosen panel area (e.g. 5-20 % panel area for EIW). Restore masonry wall using new bricks. Remove plaster along main cracks (a strip of 0.4 m width across each crack). Repair damaged area by patching new plaster using fiber-glass reinforcing mesh embedded in the base coat. Restore furnishings, electrical and plumping systems as necessary. Paint each side.
DS3	Demolish existing wall and construct new wall. Re-install existing frame (if any)	Install scaffolding and shoring systems. Remove furnishings, electrical and plumbing systems, as necessary. Remove existing window/French window (if any). Demolish existing wall. Build new infill/partition. Re-install existing window/French window (if any) or new door (if any). Restore furnishings, electrical and plumping systems as necessary. Paint each side.
DS4	Demolish existing wall and construct new wall. Install new frame (if any)	Install scaffolding and shoring systems. Remove furnishings, electrical and plumbing systems, as necessary. Demolish existing wall. Build new infill/partition. Install new window/French window or door (if any). Restore furnishings, electrical and plumping systems as necessary. Paint each side.

damage states in individual components. As a consequence, in this study the simplified approach described below has been followed to derive loss functions for masonry infills.

First of all, each damage state has been univocally associated with a set of specific repair activities that would be required to restore the masonry infill to its pre-earthquake (essentially undamaged) state. Generally speaking, the repair method depends on the attained DS (see second column of Table 5). At DS1, for instance, plaster cracks are repaired by patching new plaster, using fiberglass reinforcing mesh embedded in the base coat, on both sides of the wall. At DS2, in addition to repairing cracks, damaged bricks are removed and replaced by new bricks connected to the undamaged bricks. At DS3 and DS4 the wall is demolished and then re-built. Most of the repair activities are common for all the FGs while differing passing from one DS to another, due to the extent and/or severity of damage (see third column of Table 5). It is worth noting that repair activities imply a number of preliminary and supplementary activities that are needed to implement the actual repair actions. They include:

• ***Safety operations***, which involve a number of preliminary operations carried out for safety reasons, such as: access protection, application of curtains against dust, installation of scaffoldings and/or work platforms, etc.

• ***Demolition***, which includes removal of plaster across main cracks (a strip of 0.2 m width for DS1 and 0.4 m for DS2 should be suitable), demolition of damaged bricks (e.g., 10% of panel area for EIW at DS2) and isolation of mechanical, electrical and plumbing systems, as necessary.

• ***Cleaning***, which consists in cleaning the area adjacent to the main cracks to be repaired, removing of debris, etc.

• ***Restoring***, which consists in restoring infill/partition finishing (including ceramic tiles and skirting), electrical and plumbing distribution systems, and frames (windows, French windows and doors).

• ***Technical Costs***, which includes fees for structural engineer, project engineer, construction manager, etc.. In this study, they are assumed of the order of 8% the total cost of the intervention.

Methods of repair considered in the study, for each DS, are summarized in Table 5, together with a description of the related repair activities (including the necessary preliminary and supplementary activities). The unit costs (c_k) of the main repair actions required for each DS are listed in Table 6. They have been estimated considering the Price List for Public Works in Basilicata Region, Italy (2013). Reference to the same document has been also made to estimate the additional costs related to all the necessary preliminary and supplementary activities. Within this context, further improvements and refinements could be achieved, for instance, by surveying different building contractors to get more practical estimates of repair costs.

Considering the total costs associated with repairing of masonry infill walls, loss functions can be expressed, again in a normalized form, as follows

$$L_j|DS_i = \frac{TC_j|DS_i}{b_j \cdot A} \tag{6}$$

where $L_j|DS_i$ is the total economic loss for the j-th component conditioned on the occurrence of the i-th damage state; $TC_j|DS_i$ is the total repair cost for the j-th component when the i-th damage state has occurred; b_j is the nominal cost per square meter for a new masonry infill (or partition) with the same characteristics (including the cost of the frame (if any), plaster, ceramic tiles (if any), skirting, incidence of electrical and plumping distribution systems) and A is the gross area of the masonry wall.

Table 6 Unit costs of repair actions required for each damage state of masonry infills

Damage state	Repair Action	Unit	Cost/Unit (€/u)
DS1 (Light cracking)	Remove plaster along the upper (lateral) edge of the infill and across main diagonal cracks	m^2	7.00
	Prepare masonry surface (brushing, low-pressure water cleaning, etc.)	m^2	1.29
	Apply fiber glass plaster reinforcing mesh on each side of the wall	m^2	4.38
	Patch new plaster	m^2	25.51
	Paint	m^2	20.73
DS2 (Extensive cracking)	Remove broken and chipped bricks (if any)	m^3	49.92
	Restore infill/partition using new bricks	m^2	61.86/25.98
	Remove plaster along the upper and lateral edge of the infill and across main diagonal cracks	m^2	7.00
	Prepare masonry surface (brushing, low-pressure water cleaning, etc.)	m^2	1.29
	Apply fiber glass plaster reinforcing mesh on each side of the wall	m^2	4.38
	Patch new plaster	m^2	25.51
	Paint	m^2	20.73
DS3 (Corner Crushing)	Remove window or french window (if any)	m^2	17.41
	Remove door (if any)	m^2	6.85
	Demolish damaged infill/partition	m^3	49.92
	Build new infill/partition	m^2	61.86/25.98
	Re-install existing window or french window (if any)	m^2	22.96
	Install new door (if any)	m^2	202.98
	Apply fiber glass plaster reinforcing mesh on each side of the wall	m^2	4.38
	Patch new plaster	m^2	25.51
	Paint	m^2	20.73
DS4 (Collapse)	Remove window or french window (if any)	m^2	17.41
	Demolish damaged Infill	m^3	49.92
	Rebuild Infill	m^2	61.86
	Install new windows or french windows (if any)	m^2	318.84
	Apply fiber glass plaster reinforcing mesh on each side of the wall	m^2	4.38
	Patch new plaster	m^2	25.51
	Paint	m^2	20.73

Standard (basically average) cost ratios have been derived in an attempt to extend the applicability of the results found in this study to as many situations as possible. Standard cost ratios have been developed based on quantity surveying of a number of pre-70 RC buildings, featuring (i) exterior masonry infills realized using hollow clay bricks arranged in two single walls of 100mm thickness each, separated by a cavity of 100mm, with plan dimensions ranging from 4 m×2.75 m to 5 m×2.75 m, (ii) interior masonry partitions, realized using 100mm thickness hollow clay bricks, with plan dimensions ranging from 1.5 m×3 m to 5.5 m×3 m and (iii) pine-wood frames with plan dimensions of 1.2 m×2.2 m (French windows), 0.9 m×1.5 m (windows) and 0.9

m×2.2 m (doors), respectively.

From a statistical point of view, the standard repair cost ratios derived from the aforesaid quantity surveying can be deemed a fair estimate of the expected values of economic losses (i.e., the 50th percentile level of total repair costs), which are appropriate for estimating economic losses for typical pre-70 RC buildings. The standard repair cost ratios ($L_{FGj,DSi}(50^{th})$) reported in Table 7 are then defined as the average of the total repair costs (including all the preliminary and supplementary activities necessary to realize the intervention) for the *j*-th fragility group (EIW, IP, EIW_w, etc.), due to the attainment of the *i*-th damage state, normalized by the cost for a new masonry infill or partition with same characteristics

$$L_{FGj,DSi}\left(50^{th}\right) = AVERAGE\left(\frac{\alpha \cdot \sum_{k} c_k u_k}{b_j \cdot A}\right) \tag{7}$$

where c_k is the unit cost for the *k*-th repair action (see Table 6), u_k is the associated quantity or extension of damage for the *j*-th fragility group, *k* is the total number of repair actions necessary for that damage state; α is a cost factor which accounts for preliminary and supplementary activities not considered in Table 6 (e.g., technical costs, scaffolding, waste disposal, etc.); b_j is the nominal cost per square meter for a new masonry infill (or partition) with the same characteristics and *A* is the gross area of masonry walls. Based on the results of this study, the cost factor α ranges from about 1.6 to 2 for masonry infills and from about 2 to 2.5 for masonry partitions.

The breakdown of the standard repair cost ratios in different cost items (i.e., repairing, safety, demolition, etc.) is shown in Fig. 6, to point out the contribution of each activity to the total repair cost of masonry infills and partitions. As expected, total repair costs tend to increase while increasing the severity and extension of damage, passing from approximately 20% (for masonry infills at DS1) to approximately 150-180% (for masonry infills at DS4) of the construction cost for a new infill with the same characteristics. It is worth noting that preliminary and supplementary activities still represent the most important cost items at DS1 while they tend to become less important at DS4.

While $L_{FGj,DSi}(50^{th})$ provides information on the expected values of economic losses (i.e., essentially average losses) that can occur in masonry infills and partitions due to earthquake damage, they do not provide information on how large these losses can become in a given scenario. In other words, they do not provide information on the dispersion around those average losses. In order to improve the evaluation of expected losses, the 10^{th} and 90^{th} percentile levels of the total repair costs have been estimated, based on engineering judgment. In particular, they have been obtained multiplying the 50^{th} percentile estimate by a factor 0.5 and 2, respectively, in accordance with FEMA P-58 recommendations.

Cumulative normal distributions of the total repair cost ratios ($L_{FGj}|DS_i$) have been then derived, by fitting the 10^{th}, 50^{th}, and 90^{th} percentile estimates (see Fig. 7). The resultant median $\lambda_{FGj,DSi}$ and dispersion $\beta_{FGj,DSi}$ are reported in Table 7, for each component type and associated DS. As can be seen in Table 7, the total cost for repairing damaged masonry walls remains below 1/2 the construction cost at DS1 and DS2 while it results larger than the construction cost of a new panel with same characteristics at DS3 and DS4, mainly due to the extra costs related to demolition and disposal.

The median $\lambda_{FGj,DSi}$ and dispersion $\beta_{FGj,DSi}$ can be effortlessly implemented in PACT for PBEE analysis of RC frame buildings. To this end, a proper unit of measurement (e.g., square meter, linear meter or number of equivalent panels) must be first selected. Then, in line with

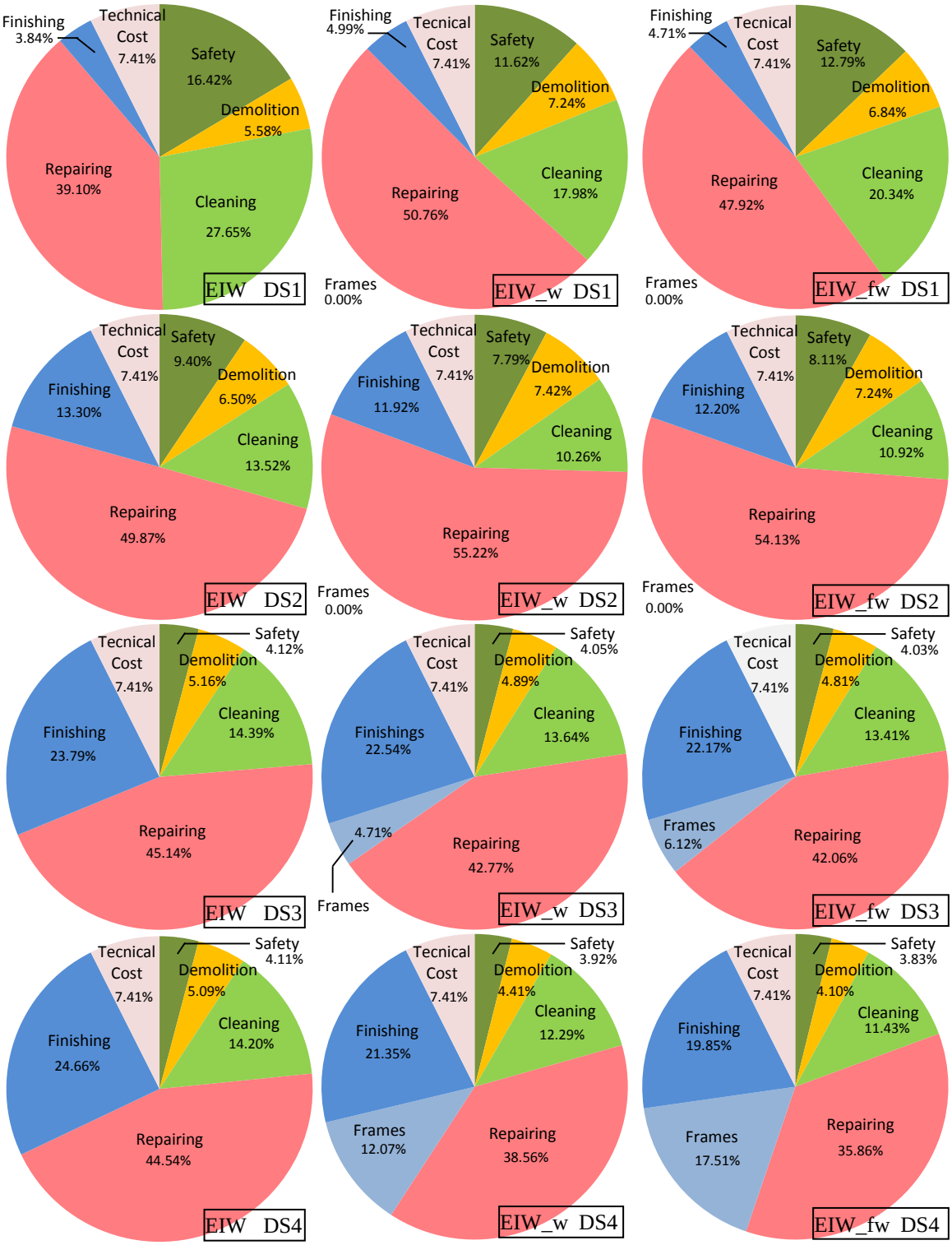

Fig. 6 Disaggregation of total repair cost ratios for infill masonry walls with and without openings

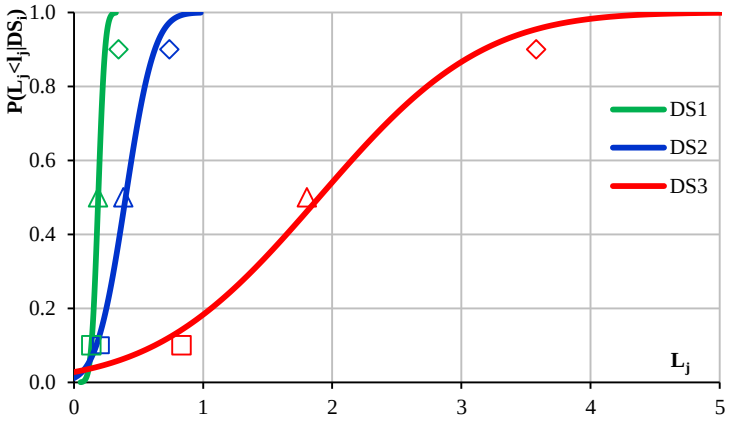

Fig. 7 Cumulative normal distributions derived by fitting 10th, 50th, and 90th percentile estimates of the total repair cost ratios for masonry infill walls (without opening), at different DSs

Table 7 Loss function parameters for performance-based seismic assessment of masonry infills and partitions

Component type	Damage State	$L_{FGj,DSi}(50^{th})$	$\lambda_{FGj,DSi}$	$\beta_{FGj,DSi}$	λ_{max}	λ_{min}	q_{max}	q_{min}
EIW	DS1	0.19	0.19	0.22	0.24	0.15	20	5
	DS2	0.38	0.40	0.44	0.48	0.34	20	5
	DS3	1.81	1.90	0.44	2.28	1.61	20	5
	DS4	1.83	1.92	0.52	2.30	1.64	20	5
EIW_w	DS1	0.19	0.19	0.22	0.24	0.15	20	5
	DS2	0.38	0.40	0.44	0.41	0.29	20	5
	DS3	1.81	1.90	0.44	1.56	1.10	20	5
	DS4	1.83	1.92	0.52	1.73	1.22	20	5
EIW_fw	DS1	0.17	0.17	0.28	0.22	0.13	20	5
	DS2	0.31	0.32	0.46	0.39	0.27	20	5
	DS3	1.25	1.32	0.46	1.58	1.12	20	5
	DS4	1.47	1.55	0.52	1.86	1.31	20	5
IP	DS1	0.22	0.22	0.19	0.28	0.17	20	5
	DS2	0.41	0.43	0.45	0.52	0.37	20	5
	DS3	1.87	1.96	0.45	2.35	1.66	20	5
IP_d	DS1	0.18	0.18	0.25	0.24	0.15	20	5
	DS2	0.33	0.34	0.46	0.41	0.29	20	5
	DS3	1.34	1.40	0.46	1.68	1.19	20	5

the recommendation of FEMA P-58 (ATC, 2012a, b), a lower/upper quantity (q_{min}/q_{max}) below/above which there is no discount reflecting economies of scale or efficiencies in operation and the associated maximum/minimum normalized repair cost ratios ($\lambda_{max}/\lambda_{min}$) shall be defined. Values of q_{min}/q_{max} (expressed in terms of number of equivalent panels) and $\lambda_{max}/\lambda_{min}$ are reported in Table 7. The corresponding normalized loss functions are shown in Fig. 8. Loss functions to be

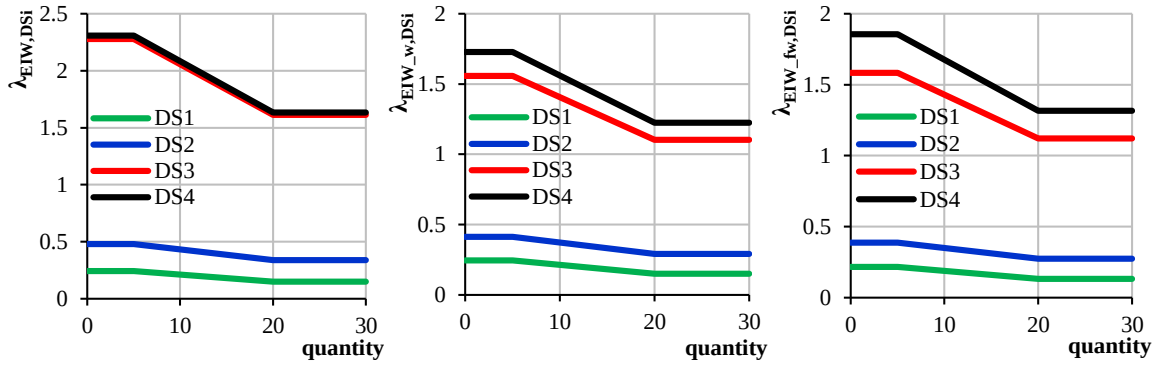

Fig. 8 Loss functions to be implemented in PACT for (a) EIW (b) EIW_w and (c) EIW_fw

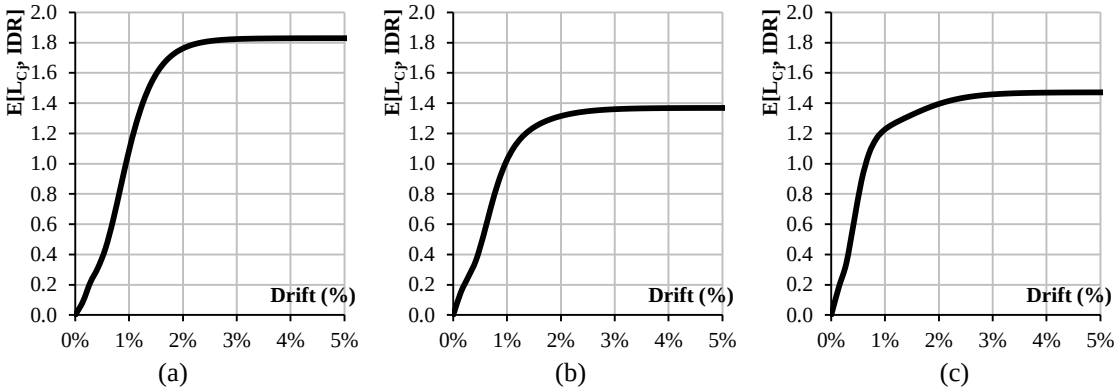

Fig. 9 Variations of the expected loss for (a) EIW, (b) EIW_w, (c) EIW_fw, as a function of IDR

implemented in PACT are obtained multiplying the total repair cost ratios $\lambda_{max}/\lambda_{min}$ by the nominal construction cost for a new infill expressed in the selected unit of measurement.

The normalized expected loss for the *j*-th fragility group ($E(L_{Cj},IDR_k)$) can be computed as the product of the median values of the distribution of the total repair cost ratios associated with each DS (see Table 7) by the probability of being in each DS (see Fig. 2)

$$E\left(L_{Cj}, IDR_k\right) = \sum_{i=1}^{m} \lambda_{FGj,DSi} \cdot P\left(DS = ds_i, IDR_k\right) \tag{8}$$

where m=4 is the number of damage states and $P(DS=ds_i, IDR_k)$ is the probability of the component being in the *i*-th damage state when it is subjected to a peak interstory drift ratio IDR_k. Fig. 9 shows the normalized expected loss for masonry infills, as a function of the peak interstory drift ratio attained during an earthquake.

7. Conclusions

In this study, fragility functions for exterior masonry infills and interior partitions have been

tentatively derived, based on results of previous experimental studies. The attention has been focused on masonry infills realized with hollow clay bricks and pine-wood frames with ordinary plan dimensions. Repair costs for damaged masonry walls have been estimated based on accurate quantity surveying of a number of pre-70 RC buildings, using official costing manuals for Italy. Finally, loss functions, that provide expected economic losses for individual exterior masonry infills and interior partitions, as a function of the experienced peak interstory drift ratios, have been developed. The fragility and loss functions derived in this study can be directly implemented in the Performance Assessment Calculation Tool (PACT) of FEMA P-58 for PBEE analysis of RC frame buildings.

Further improvements and refinements in the estimation of fragility curves and loss functions for exterior masonry infills and interior masonry partitions may be achieved by addressing the following issues:

• Derive more accurate estimates of fragility parameters for masonry infills and partitions with openings, based on the experimental results of further laboratory tests and field survey of post-earthquake damage;

• Derive different fragility parameters for exterior interior (not-infilled) partitions, based on the results of further experimental studies and expert opinion;

• Infill typology can affect the fragility parameters of masonry infills (and partitions). As a consequence, whenever possible and practical, efforts shall be made to consider the masonry infill typology, distinguishing at least two types of masonry infills, i.e., solid clay brick infills and clay brick infills with vertical holes;

• Define fragility parameters for masonry infills as a function of the apparent axial strain of an equivalent single-diagonal strut model (in lieu of the interstory drift ratio). This is because the equivalent single-diagonal strut model is commonly used for the analytical representation of masonry infills and recent studies by Hak *et al*. (2012) has indicated that the drift capacity can be directly related to the aspect ratio of the infill and apparent strain capacity of the equivalent diagonal strut model. Using the concept of apparent strain capacity, diagonal strain-based fragility functions could be defined;

• The accuracy of the loss functions developed in this study may be further improved by surveying different building contractors to get more practical estimates of repair costs.

Acknowledgements

This work has been carried out within the Line 7 of the ReLUIS/DPC 2014-2018 research program, dealing with direct displacement approaches for the evaluation of seismic losses of buildings in pre- and post- rehabilitation conditions. The authors gratefully acknowledge the support of the RELUIS Consortium for this research.

References

Angel, R., Abrams, D., Shapiro, D., Uzarski, J. and Webster M. (1994), "Behavior of reinforced concrete frames with masonry infills", *Civil Engineering Studies*, Structural Research Series N. 589, UILU-ENG-942005, Dept. of Civil Engineering, University of Illinois at Urbana Champaign.

ATC - Applied Technology Council (2012a), *FEMA P-58 Next-generation Seismic Performance Assessment for Buildings, Volume 1 - Methodology*, Federal Emergency Management Agency, Washington, DC.

ATC - Applied Technology Council (2012b), *FEMA P-58 Next-generation Seismic Performance Assessment for Buildings, Volume 2 - Implementation Guide*, Federal Emergency Management Agency, Washington, DC.

BUR (Official Journal of Regione Basilicata) (2013), *Price List of Public Works in Basilicata Region*, Potenza. (in Italian)

Bozorgnia, Y. and Bertero, V.V. (2004), *Earthquake Engineering: From Engineering Seismology to Performance-Based Earthquake Engineering*, CRC Press.

Calvi, G.M., Bolognini, D. and Penna, A. (2004), "Seismic performance of masonry-infilled R.C. frames: benefits of slight reinforcements", *Sismica 2004, Congreso National de Sismologia e Engenharia Sísmica*, Guimaraes, Portugal.

Carydis, P.G., Mouzakis, H.P., Taflambas, J.M. and Vougioukas, E.A. (1992), "Response of infilled frames with brick walls to earthquake motions", *Proceedings of the 10th World Conference on Earthquake Engineering*, Madrid.

Carvalho, E.C. and Coelho, E. (2001), "Seismic assessment, strengthening and repair of structures", *ECOEST2-ICONS report n. 2*, European Commission - Training and Mobility of Researchers Program.

Colangelo, F (2003), "Experimental evaluation of Member-by-Member models and damage indices for infilled frames", *J. Earthq. Eng.*, **7**(1), 25-50.

Dolsek, M. and Fajfar, P. (2008), "The effect of masonry infills on the seismic response of a four-storey reinforced concrete frame-a deterministic assessment", *Eng. Struct.*, **30**(7), 1991-2001.

Hak, S., Morandi, P., Magenes, G. and Sullivan, T.J. (2012), "Damage control for clay masonry infills in the design of RC frame structures", *J. Earthq. Eng.*, **16**(1), 1-35.

Kakaletsis, D.J. and Karayannis, C.G. (2008), "Influence of masonry strength and openings on infilled R/C frames under cyclic loading", *J. Earthq. Eng.*, **12**(2), 197-221.

Kappos, A.J., Stylianidis, K.C. and Michailidis, C.N. (1998), "Analytical models for brick masonry infilled r/c frames under lateral loading", *J. Earthq. Eng.*, **2**(1), 59-87.

Lilliefors, H. (1967), "On the Kolmogorov-Smirnov test for normality with mean and variance unknown", *J. Am. Statist. Assoc.*, **62**(318), 399-402.

Manos, G.C., Triamataki, M. and Yasin, B. (1995), "Experimental and numerical simulation of the influence of masonry infills on the seismic response of reinforced concrete framed structures", *Proceedings of the 10th European Conference on Earthquake Engineering*, Eds. A.A. Balkema, Rotterdam, **3**, 1513-1518.

Mehrabi, A.B., Shing, P.B., Schuller, M.P. and Noland, J.L. (1996), "Experimental evaluation of masonry infilled RC frames", *J. Struct. Eng.*, ASCE, **122**(3), 228-237.

Mosalam, K.M., White, R.N. and Gergely, P. (1997), "Static response of infilled frames using quasi-static experimentation", *J. Struct. Eng.*, ASCE, **123**(11), 228-237.

Negro, P. and Verzeletti, G. (1996), "Effect of infills on the global behavior of R/C frames: Energy considerations from pseudodynamic tests", *Earthq. Eng. Struct. Dyn.*, **25**(8), 753-773.

Paulo Pereira, M.F., Neto Pereira, M.F., Dias Ferreira, J.E. and Lourenço, P.B. (2011), "Behavior of masonry infill panels in RC frames subjected to in plane and out of plane loads", *Proceedings of the 7th Amcm International Conference*, Krakow, Poland.

Pires, F. and Carvalho, E.C. (1992), "The behaviour of infilled reinforced concrete frames under horizontal cyclic loading", *Proceedings of the 10th World Conference on Earthquake Engineering*, Madrid.

Pujol, S., Benavent-Climent, A., Rodriguez, M.E. and Smith-Pardo, J.P. (2008), "Masonry infill walls: An effective alternative for seismic strengthening of low-rise Reinforced Concrete building structures", *The 14th World Conference on Earthquake Engineering*, Beijing, China.

Ross, S.M. (2003), "Peirce's criterion for the elimination of suspect experimental data", *J. Eng. Technol.*, **20**(2), 38-41.

Sigmund, V. and Penava, D. (2012), "Experimental study of masonry infilled R/C frames with opening", *Proceedings of the 15WCEE*, Lisbon, Portugal.

Schneider, S.P., Zagers, B.R. and Abrams, D.P. (1998), "Lateral strength of steel frames with masonry infills having large opening", *J. Struct. Eng.*, ASCE, **124**(8), 896-904.

Sucuoglu, H. (2013), "Implications of masonry infill and partition Damage in performance perception in

residential buildings after a moderate earthquake", *Earthq. Spectra*, **29**(2), 661-667.
Tasnimi, A.A. and Mohebkhah, A. (2011), "Investigation on the behavior of brick-infilled steel frames with openings, experimental and analytical approaches", *Eng. Struct.*, **33**(3), 968-980.
Zarnic, R. (1995), "Modelling of response of masonry infilled frames", *Proceedings of the 10th European Conference on Earthquake Engineering*, Eds. A.A. Balkema, Rotterdam, **3**, 14811486.
Zarnic, R. and Gostic, S. (1997), "Masonry infilled frames as an effective structural sub assemblage", *Proceedings of the International Workshop on Seismic Design Methodologies for the next generation of codes*, Bled, Slovenia.
Zarnic, R. and Tomazevic, M. (1984), "The behaviour of masonry infilled reinforced concrete frames subjected to cyclic lateral loading", *Proceedings of the 8th World Conference on Earthquake Engineering*, San Francisco, Prentice-Hall, New Jersey.

SA